

NOVEMBER 14, 2019

VOLUME 123

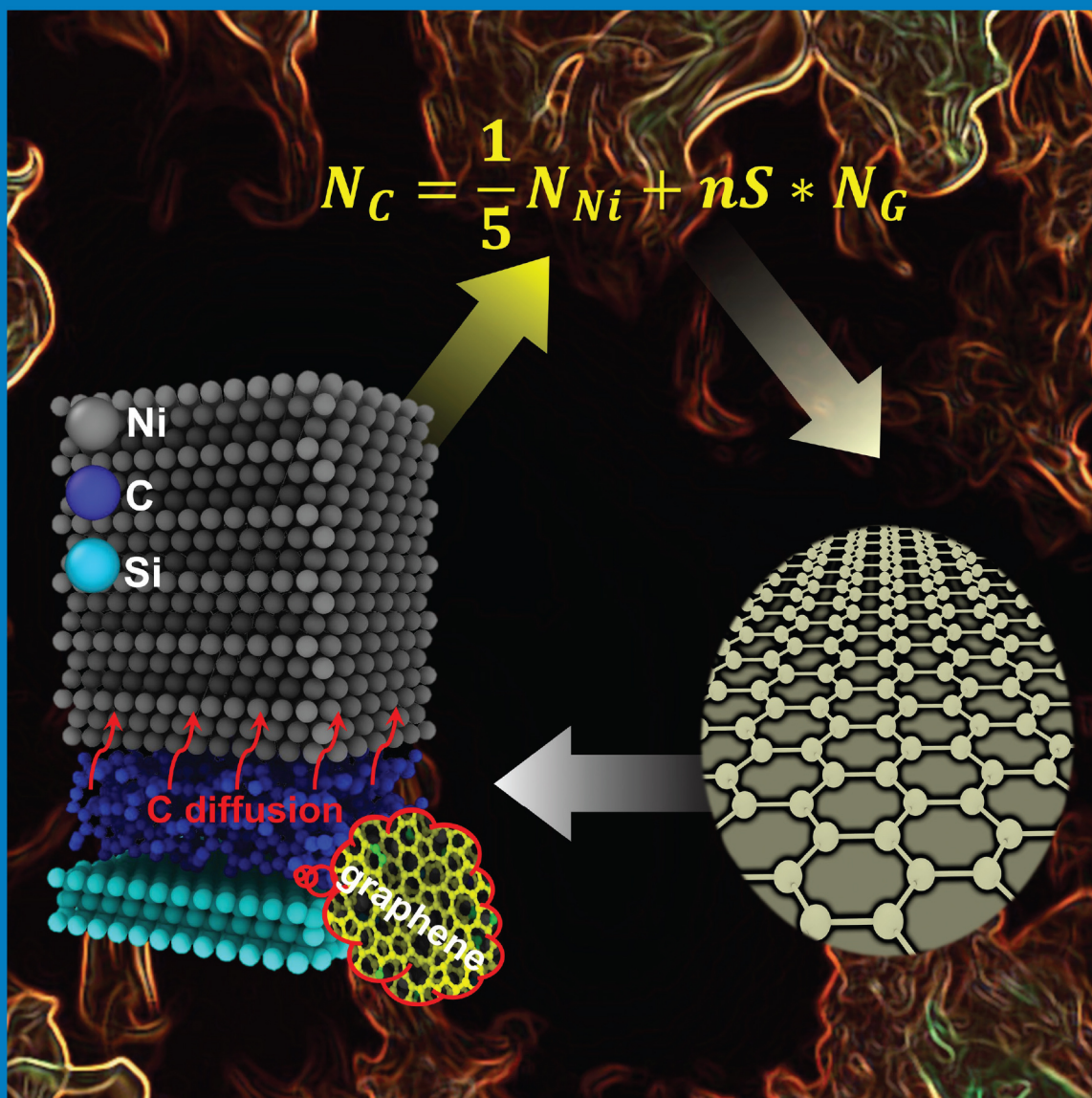
NUMBER 45

pubs.acs.org/JPCC

THE JOURNAL OF PHYSICAL CHEMISTRY

C

Fast Synthesis of Graphene with Desired Structure via Ni-Catalyzed Transformation of Amorphous Carbon during Rapid Thermal Processing



ENERGY CONVERSION AND STORAGE; CATALYSIS; OPTICAL, ELECTRONIC,
AND MAGNETIC PROPERTIES AND PROCESSES; INTERFACES;
NANOMATERIALS AND HYBRID MATERIALS



ACS Publications
Most Trusted. Most Cited. Most Read.

www.acs.org

Fast Synthesis of Graphene with a Desired Structure via Ni-Catalyzed Transformation of Amorphous Carbon during Rapid Thermal Processing: Insights from Molecular Dynamics and Experimental Study

Xiaowei Li,^{*,†,‡,§} Zhenyu Wang,[‡] Hanchao Li,^{‡,§} Aiying Wang,^{*,‡,||} and Kwang-Ryeol Lee^{*,†}

[†]Computational Science Center, Korea Institute of Science and Technology, Seoul 136-791, Republic of Korea

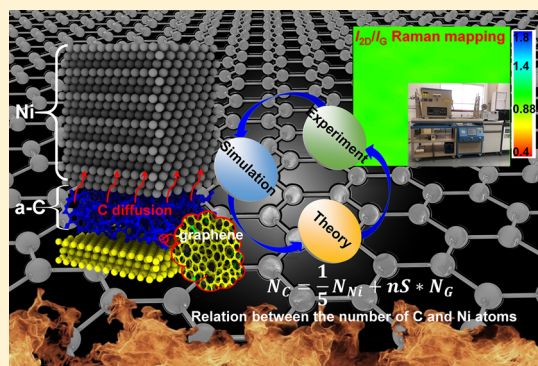
[‡]Key Laboratory of Marine Materials and Related Technologies, Zhejiang Key Laboratory of Marine Materials and Protective Technologies, Ningbo Institute of Materials Technology and Engineering, Chinese Academy of Sciences, Ningbo 315201, P. R. China

[§]School of Physical Science and Technology, ShanghaiTech University, Shanghai 201210, P. R. China

^{||}Center of Materials Science and Optoelectronics Engineering, University of Chinese Academy of Sciences, Beijing 100049, P. R. China

Supporting Information

ABSTRACT: Fast transfer-free synthesis of graphene on a given dielectric substrate is achieved by Ni-catalyzed solid-state transformation of amorphous carbon (a-C) through rapid thermal processing (RTP). Nevertheless, the dependence of this transformation behavior on Ni/a-C thickness and the underlying mechanism at the atomic scale are not well comprehended, leading to the lack of efficient synthesis and modulation of the graphene structure experimentally. Here, using reactive molecular dynamics simulation, we select Ni as a catalyst and present a systematic investigation of the diffusion of C into Ni and the corresponding structural transformation of a-C into graphene under different conditions. The results emphasize the decisive role of the Ni/C atomic ratio in the quality and layer number of graphene instead of the Ni or a-C thickness. Combined with the results during the cooling process, they suggest that the a-C-to-graphene transformation mechanism is mainly dependent on the diffusion behavior of C and the catalytic effect of Ni, rather than the dissolution/precipitation. Most importantly, both the simulation and experiment propose a universal equation to elucidate the relationship between the number of C and Ni atoms and the RTP graphene structure. This finding not only enables the fast synthesis and modulation of a-C-transformed graphene with the desired structure and layers on various substrates without the transfer process but also gets rid of the limitation of carbon sources and Ni structures and simplifies the RTP process parameters significantly, which can be utilized widely in experiment to promote the commercial application of graphene.



1. INTRODUCTION

Graphene, a two-dimensional material connected by sp^2 hybridized bonds, has become increasingly popular in both scientific and industrial developments because of its superior mechanical and electrical properties,^{1–5} being a strong candidate for applications in next-generation electronics, sensors, and solar cells.^{6,7} To date, various attempts,^{8–13} such as chemical vapor deposition (CVD),^{12,13} have been adopted for growing graphene with high quality. Interestingly, recent studies^{14–18} developed a metal-catalyzed solid transformation of amorphous carbon (a-C) into graphene by a rapid thermal processing (RTP) strategy, by which high-quality graphene was synthesized on a desired dielectric substrate (Si or SiO_2) directly without a transfer process. This not only diminishes the degradation of graphene caused by wrinkling,

cracking, and contamination to the graphene structure but also boosts the potential commercial application of RTP graphene because a-C has a flexible structure and is available to various substrates at room temperature on a large scale.^{19,20}

Xiong et al.¹⁶ have reported that the thickness of a-C and the Ni catalyst significantly affected the transformation of a-C into graphene during the RTP process and tailored the layers and quality of the generated graphene structure. However, a fundamental understanding of the thickness dependence of the a-C-to-graphene transformation (diffusion behavior of C atoms, evolution of the a-C structure, and graphene quality)

Received: May 30, 2019

Revised: July 30, 2019

Published: July 31, 2019

on the atomic scale is still lacking, which is required to settle the controversy on the potential mechanism in experiment, such as dissolution/precipitation^{14,18,21} or metal-induced crystallization.^{4,15,16,22} Furthermore, due to the diversity of a-C (tetrahedral a-C, graphite-like carbon, etc.)^{19,20} or the existence of Ni defects (polycrystalline, vacancy, etc.), the structures may have the same thickness but largely different number of atoms. Hence, the thickness relationship between the a-C and Ni layers only provides limited information for the effective synthesis of RTP graphene, and thus a trial-and-error strategy is still the dominant route for the synthesis of high-quality RTP graphene in experiment. To realize goal-oriented fabrication of a-C-transformed graphene for technical applications, exploring the fundamental relationship of the RTP graphene structure with the number of C and Ni atoms, rather than a-C and Ni thickness, is a prerequisite.

In this work, we also select Ni as the catalyst and conduct reactive molecular dynamics (RMD) simulations to gain insight into the a-C-to-graphene transformation during the RTP process. The dependence of the diffusion behavior of C, structural transformation of both Ni and a-C, and the bond structure of the formed graphene on different Ni/C ratios is systematically evaluated. The derivation of a universal equation for the relationship between the number of C and Ni atoms and the graphene structure is provided, which drives the successful and fast fabrication of graphene with a desired structure in experiment. These results disclose the underlying a-C-to-graphene transformation mechanism and can serve as a promising guidance for the goal-oriented design and manipulation of various graphene structures, such as mono- or multilayered structures, on various conductive or dielectric substrates without a transfer process.

2. COMPUTATIONAL AND EXPERIMENTAL METHODS

2.1. Ni@a-C Simulation Model and Related Parameters. All calculations were carried out by the Large-scale Atomic/Molecular Massively Parallel Simulator.²³ Figure 1 shows the three-dimensional simulation model consisting of bottom a-C and upper Ni(111) layers (Ni@a-C). Following a

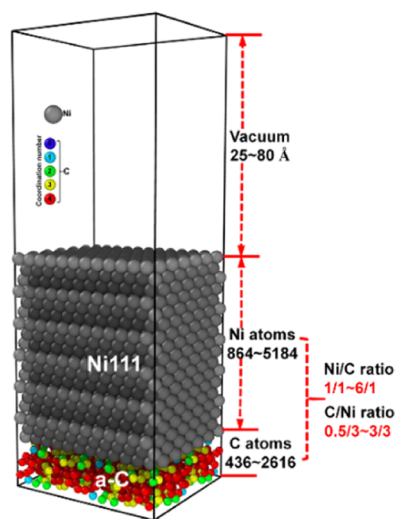


Figure 1. Ni@a-C model used in this work, in which the numbers of C and Ni atoms were tailored to obtain the different Ni/C or C/Ni ratios.

previous study,²⁴ the a-C structure obtained by ab initio MD simulations,²⁵ which had a high density of 3.22 g/cm³, sp³ fraction of 63.3 atom %, and sp² fraction of 25.7 atom %, was adopted as an optimal candidate of carbon source. The Ni(111) surface containing 144 atoms per atomic layer was considered as the catalyst because of its relatively higher diffusion barrier for C into the Ni structure than Ni(100) and Ni(110) surfaces, as confirmed by our previous calculation.²⁶ By tailoring the number of C (436–2616) and Ni (864–5184) atoms, different Ni/C (1/1–6/1) or C/Ni (0.5/3–3/3) atomic ratios were achieved. The corresponding average lattice mismatch between the Ni(111) and a-C models was 2.6% in the *x*-direction and 0.6% in the *y*-direction. There was no fixed layer in the simulation,²⁷ and a vacuum space (25–80 Å) was employed in the direction perpendicular to the Ni(111) surface; the time step was 0.25 fs, and periodic boundary conditions were employed along the *x* and *y* directions.

A stepwise heating strategy^{27,28} was used to increase the temperature from 300 to 1800 K by the NVT ensemble using a Nosé–Hoover thermostat,²⁹ and then the system was relaxed at 1800 K for 1350 ps to study the a-C-to-graphene transformation. A previous study²⁴ revealed that 1800 K was suitable to observe the obvious diffusion behavior during the short MD simulation time without serious graphitic dissolution, although the absence of Ni defects or surface/interface contamination made the temperature higher than those in previous experiments.^{14–18} In addition, the cutoff values, R_{cut} for judging whether the bond formed or not²⁴ were 1.85 Å for C–C, 2.45 Å for C–Ni, and 3.25 Å for Ni–Ni, respectively, by the radial distribution function (RDF).²⁵ The ReaxFF potential developed by Mueller et al.³⁰ was employed to describe the interactions between the C and Ni atoms, which has been validated by previous results.²⁶

2.2. Experimental Preparation and Characterization of RTP Graphene. The Ni@a-C samples were prepared by the magnetron sputtering method with a high-purity graphite target (99.99%) for a-C deposition and a Ni plate target (99.95%) for Ni deposition, respectively, on a SiO₂/Si wafer as the substrate with a size of 2 × 5 cm². During the film deposition process, Ar gas was introduced into the sputtering target, and the DC negative bias voltage for the substrate was –150 V; the deposition times were 1 min for the a-C film and 1.375 min for the Ni film separately. Then, the RTP process was conducted for the samples on a Rapid Thermal Processor (Otf-1200x) in a vacuum environment at a temperature of 1223 K,^{4,14} after maintaining at that temperature for 1, 6, and 18 min separately, the samples were cooled to room temperature in about 20 min. Finally, the top Ni layer was etched away in a 3 mol/L HCl solution, and then Raman mapping images of the obtained graphene films were recorded on a Renishaw inVia Raman microscope with 532 nm (2.33 eV) laser excitation.

3. RESULTS AND DISCUSSION

3.1. Dependence of the a-C-to-Graphene Transformation on Ni/C or C/Ni Atomic Ratios. In the Ni@a-C systems, the effect of different Ni/C atomic ratios (1/1–6/1) on the a-C-to-graphene transformation is first investigated, as illustrated in Figure 2, in which the number of Ni atoms is tailored from 864 to 5184 with respect to the same number of C atoms (872). However, due to the existence of defects in the a-C-transformed graphene structure during the short MD simulation, it is defined as graphene-like carbon (GLC), which

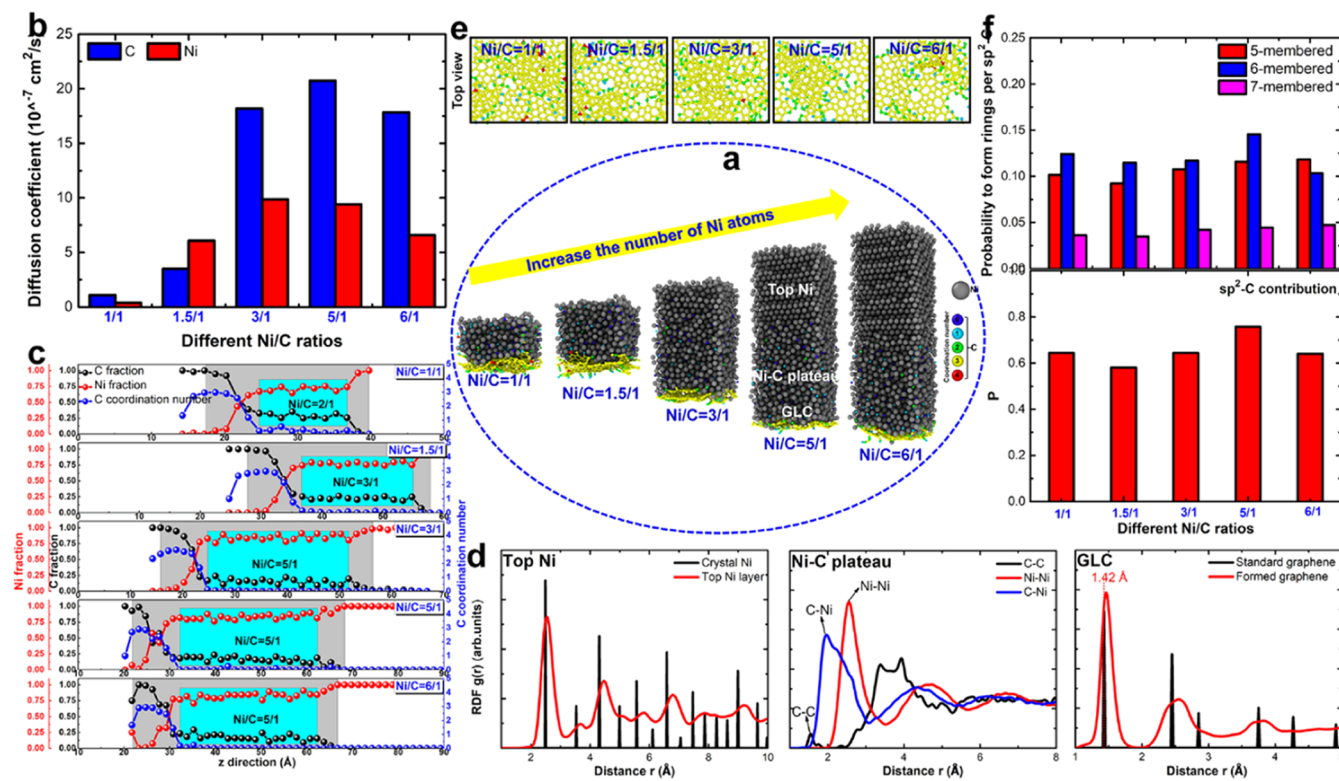


Figure 2. Results for systems with different Ni/C ratios obtained by tailoring the number of Ni atoms with respect to the same number of C atoms (RTP conditions: temperature – 1800 K; diffusion time – 1350 ps). (a) Final morphologies after diffusion at 1800 K for 1350 ps. (b) Diffusion coefficient of C and Ni atoms for each case. (c) Profiles of C and Ni atomic fractions along the diffusion couple direction with different Ni/C ratios of the systems after diffusion at 1800 K for 1350 ps. (d) RDF spectra for GLC, plateau region, and top Ni layer for the system with a Ni/C ratio of 5/1. (e) GLC morphologies obtained for each system. (f) Ratio of the number of rings contributed by sp^2 -C to the total number of rings and the probability of ring formation per sp^2 -C atom.

has an approximate 2D and sp^2 -dominant structure, to give it an accurate description and avoid the potential misunderstanding. Figure 2a shows that upon increasing the Ni/C atomic ratio, more C atoms diffuse into Ni layers, whereas the GLC structure tends to evolve from an incomplete bilayer to a monolayer approximately, and the surplus Ni layer still maintains a regular arrangement, agreeing well with previous reports.^{16,26} The diffusion coefficient, D , is calculated for each case by the linear fitting of the mean square displacement (MSD)–time curves,²⁶ as shown in Figure 2b. The C diffusion coefficient is strongly dependent on the Ni/C atomic ratio of the Ni@*a*-C system. When we change the Ni/C ratio from 1/1 to 5/1, the diffusion coefficient of C increases significantly from 1.1×10^{-7} to 20.7×10^{-7} cm^2/s , whereas with a further increase in the Ni/C ratio to 6/1, it drops slightly to 17.8×10^{-7} cm^2/s , being related to the corresponding evolution of the *a*-C structure during the diffusion process, as will be discussed later. Note that the change in the diffusion coefficient of Ni atoms with the Ni/C ratio is similar to that of C atoms (Figure 2b).

Due to the differences in the diffusion coefficients of C and Ni atoms, the corresponding evolution of the intermixing layer and the plateau region after diffusion at 1800 K for 1350 ps are observed in Figure 2c. With a change in the Ni/C ratio of the system from 1/1 to 6/1, the Ni/C atomic ratios in the corresponding plateau regions (light blue background in Figure 2c) are 2/1, 3/1, 5/1, 5/1, and 5/1, respectively, implying that the formed plateaus with different ratios have no obvious effect on the formation of GLC. However, it should be mentioned

that the existence of Ni is essential to stabilize the C dangling bonds, dissolution of C atoms, and catalyze and support the newly grown flat graphene.^{27,31} In particular, the Ni/C atomic ratio in the plateau region tends to be 5/1 when enough Ni atoms are supplied (see Figure S1 in Section S1 of the Supporting Information), but there is no specific phase of nickel carbide distinguished, being different from the formation of Ni_3C in Xiong's observation.¹⁶ This difference may be related to the RTP time, temperature, both the Ni and *a*-C structures, and the limited characterization in experiment.

For each case, after diffusion at 1800 K for 1350 ps, the system is divided approximately into three regions. Taking the system with a Ni/C ratio of 5/1 for example (Figure 2d), it consists of the GLC, Ni–C plateau, and top Ni layer. The RDF for GLC has three obvious peaks located at 1.46, 2.53, and 3.83 Å; the RDF for the Ni–C intermixing plateau shows a viscous liquid-like structure,^{24,27} whereas the top surplus Ni layer that does not melt completely still retains its crystalline structure with slight migration of atoms from the original equilibrium position.

The corresponding evolution of the *a*-C hybridization structures for the systems with different Ni/C ratios (see Figure S2 in Section S1 of Supporting Information) reveals that for each case the sp^3 -C fraction decreases significantly with the diffusion time, whereas the sp^2 -C fraction increases first and then decreases. However, for Ni/C ratios of 5/1 and 6/1, the final decrease in the sp^2 -C fraction is more severe than that in the other cases, owing to the high diffusion coefficient of C atoms (Figure 2b), which accelerates the re-dissolution of the

formed graphitic structures into the Ni layer, as proved by experimental²² and simulation observations.²⁴ In addition, the sp³-C fraction of a-C in the system with a Ni/C ratio of 5/1 is higher than that with a Ni/C ratio of 6/1 (see Figure S2 in Section S1 of the Supporting Information), which can account for the slight difference in the diffusion coefficient of C (Figure 2b).

To evaluate the role of the Ni/C ratio in the formation of the GLC structure, Figure 2e displays the morphology of GLC obtained for each case. We infer that as the Ni/C ratio increases, the GLC structure changes from bilayer to monolayer, because of the lower number of C atoms in the GLC side caused by the high diffusion coefficient, agreeing well with experiment.¹⁶ Moreover, with the increase in the Ni/C ratio from 1/1 to 6/1, both the hybridization structure and bond-length distribution of GLC (see Figure S3 in Section S1 of the Supporting Information) show no obvious change, indicating that tailoring the number of Ni atoms to modulate the Ni/C ratio has no distinct effect on the hybridization ratio, but the peak in the bond-angle distribution tends to split into two peaks, with one being close to 120°. If we only focus on the sp²-C structure, the number of rings, including 5-, 6-, and 7-membered ones, contributed by sp²-C is calculated, and then the ratio of this sp²-C-induced rings to the total number of rings is evaluated, as shown in Figure 2f. This indicates that when the Ni/C ratio is 5/1, the relative contribution from sp²-C is higher than in other cases; in addition, the maximal probability of ring formation per sp²-C atom is also obtained for this case (Figure 2f). Thus, we conclude that the GLC generated from the system with a Ni/C atomic ratio of 5/1 is of the best quality compared to that from other systems.

The above-mentioned results elucidate a strong dependence of a-C-to-graphene transformation on the number of Ni atoms. In addition, by fixing the number of Ni atoms at 2592, the number of C atoms is increased from 436 to 2616, to obtain different C/Ni ratios; this C/Ni ratio also plays a decisive role in the formation of RTP GLC, and the results obtained upon varying the C/Ni ratio after the RTP process are given in Figure 3 and Section S2 of the Supporting Information. The insets in Figure 3 show that when the C/Ni ratio of the system is increased from 0.5/3 to 3/1, the structure for residual C

atoms near the diffusion zone front clearly evolves from incomplete monolayer to bilayer GLC approximately, consistent with experimental results,¹⁶ but there is no obvious layered GLC generated at C/Ni ratios of 2/3 and 3/3. Upon increasing the number of C atoms, the C atoms far from the C/Ni interface are slightly affected by the Ni catalyst, and this also prohibits the structural transformation of a-C and the diffusion of C into Ni (Figure 3) by chemical bonding, resulting in more carbon atoms remaining when the C/Ni ratio of the system is 2/3 or 3/3. Hence, the formation of the GLC structure during the RTP process is more sensitive to the number of C atoms than that of Ni atoms. Furthermore, the viscous liquid-like plateau is also observed in each case (see Figures S4 and S5 in Section S2 of the Supporting Information),²⁷ with the Ni/C atomic ratios being 6/1, 6/1, 5/1, 5/1, and 5/1, as the C/Ni ratio of the system is increased from 0.5/3 to 3/3. At the C/Ni ratio of the system of 3/3 and 2/3, although the Ni/C atomic ratio of the plateau region is 5/1, the absence of RTP GLC further indicates that different Ni/C atomic ratios in the plateau regions have no direct effect on growing graphene.

3.2. Development of the Universal Equation for a-C-to-Graphene Transformation. The formation and quality of RTP graphene transformed from a-C strongly rely on the Ni/C or C/Ni atomic ratio in the Ni@a-C system, similar to the dependence of the transformation on the thickness of the a-C or Ni layers reported by Xiong et al.¹⁶ However, the above-mentioned analysis reveals that this a-C-to-graphene transformation is fundamentally dependent on the number of C and Ni atoms, rather than the thickness of the a-C or Ni layers. Therefore, from the results including the Ni/C atomic ratio of the plateau region (Figure 2c and Figure S4 in Section S2), the number of interacted Ni and C atoms (from plateau and C–Ni intermixing regions), the number of residual C atoms available for the formation of GLC, and the layers of formed GLC, a universal equation about the relationship between the number of C and Ni atoms and the RTP graphene structure, which is suitable for the a-C-to-graphene transformation during the RTP process, is derived, for the first time, as follows:

$$N_C = \frac{1}{5}N_{Ni} + nS*N_G \quad (1)$$

where the first term represents the C atoms diffused into Ni layers and the second term is the residual C atoms available for the growth of graphene; N_G is the number of C atoms per unit area required to form perfect monolayer graphene, which has a constant value of 0.382 per Å²; S is the target area for graphene in Å²; n is the desired number of graphene layers; N_{Ni} and N_C are the number of Ni and C atoms in the system, respectively.

In the present simulated systems, eq 1 can be parameterized as follows to predict the formation of intact monolayer and bilayer graphene structures:

$$N_C = \frac{1}{5}N_{Ni} + 305 \text{ For intact monolayer graphene} \quad (2)$$

$$N_C = \frac{1}{5}N_{Ni} + 610 \text{ For intact bilayer graphene} \quad (3)$$

In our previous work,²⁶ these two specified equations have successfully accounted for the transformation of a-C into graphene caused by the different Ni surfaces. Here, in Figure 4a, they further clearly describe the relationship between the number of C and Ni atoms and the GLC structure, which is

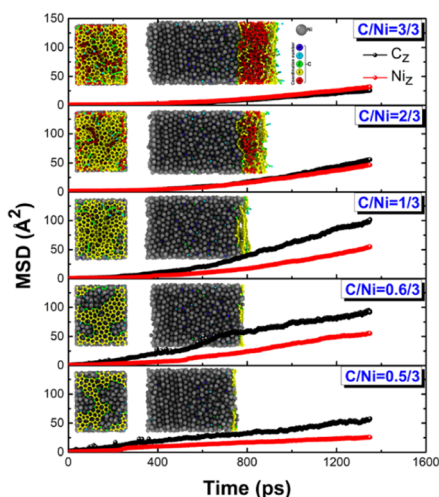


Figure 3. MSD of C and Ni atoms with different C/Ni ratios of the systems at 1800 K, in which the insets are the final morphologies after diffusion at 1800 K for 1350 ps.

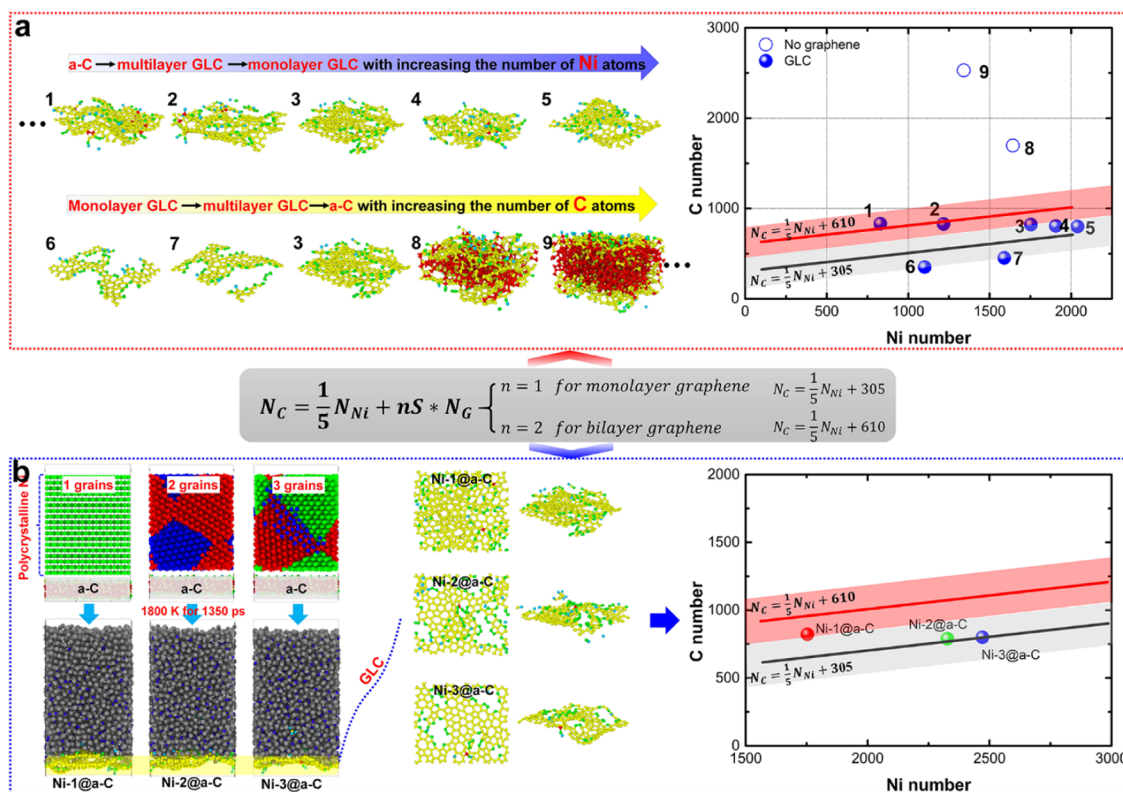


Figure 4. Relationship between the number of C and Ni atoms and the corresponding GLC structures in the present simulations when (a) the number of Ni or C atoms is increased separately to tune the Ni/C ratio or (b) the polycrystalline Ni is adopted instead of the single-crystalline one.

affected by the Ni/C or C/Ni ratios of the Ni@a-C system. If the number of C atoms is fixed, a-C with an increase in the number of Ni atoms changes from the amorphous carbon state to multilayer and monolayer graphene, which could also be reached conversely by decreasing the number of C atoms while fixing the number of Ni atoms. This universal eq 1 has been mentioned in previous experiments.^{14–18,21,22} In particular, compared to the Ni layer, the small line slope in Figure 4a also reflects higher sensitivity of RTP graphene growth to the a-C layer, coinciding with the present results in Figures 2 and 3. This has not been mentioned in the earlier calculation and experimental reports,^{14–18,21,22,24,26} providing guidance for the effective modulation of RTP graphene in experiment.

As well known, the Ni layer in experiment commonly contains many vacancies or is in a polycrystalline rather than single-crystalline state.^{14–18} It is necessary to explore the effect of Ni defects on the a-C-to-graphene transformation, because it can not only clarify the difference in diffusion behavior and RTP temperature between the simulation and experiment but also validate the universality of eq 1. Polycrystalline Ni structures containing two and three grains with random crystallographic orientation are fabricated separately to combine with the a-C structure (referred to as Ni-2@a-C and Ni-3@a-C), as shown in Figure 4b. The details of the computational method and analysis can be found in Section S3 of the Supporting Information. Interestingly, the transformation of a-C into GLC catalyzed by polycrystalline Ni can also be well described by eq 1 (Figure 4b). Upon changing the system from Ni-1@a-C to Ni-3@a-C, the a-C-transformed RTP GLC changes from bilayer to monolayer with an improved regular arrangement. This is because the presence of defects and grain boundaries in the Ni layers lowers the

diffusion barrier of C into the Ni layers, similar to previous work,²⁶ and thus leads to a significant increase in the diffusion coefficient (Figures S8 and S9 in Section S3 of the Supporting Information). Consequently, more C atoms diffuse into the Ni layers, whereas fewer C atoms remain at the bottom to grow the GLC structure. Moreover, the significantly increased diffusion coefficient induced by polycrystalline Ni also explains why the temperature in experiment^{4,14–18} is lower than that in this calculation.

3.3. Goal-Oriented Fabrication and Characterization of RTP Graphene in Experiment. Based on the relationship between the number of C and Ni atoms and RTP graphene, an experiment is carried out to validate whether the goal-oriented fabrication of graphene can be achieved according to eq 1. To tune the number of C and Ni atoms in experiment, the number of moles of deposited C or Ni atoms as a function of deposition time is established first, as shown in Figure 5a. If one supposes to fabricate bilayer graphene on a desired dielectric substrate via the RTP approach, the bottom a-C layer with 1.19×10^{-6} mol and the top Ni layer with 5.39×10^{-6} mol are successively deposited on the SiO₂ substrate. Figure 5b discloses the relation between the number of C and Ni atoms in the deposited sample (black dot), indicating that bilayer graphene should be formed after the RTP process according to eq 1.

After both RTP and Ni-etching processes, the Raman analysis of the as-grown graphene sample is undertaken, and its dependence on the RTP time is also mentioned. The corresponding Raman mappings of the 2D to G peak ratios, I_{2D}/I_G , are presented in Figure 5c. Normally, few-layered graphene with more than three layers has an I_{2D}/I_G ratio smaller than 0.8, whereas monolayer graphene can be

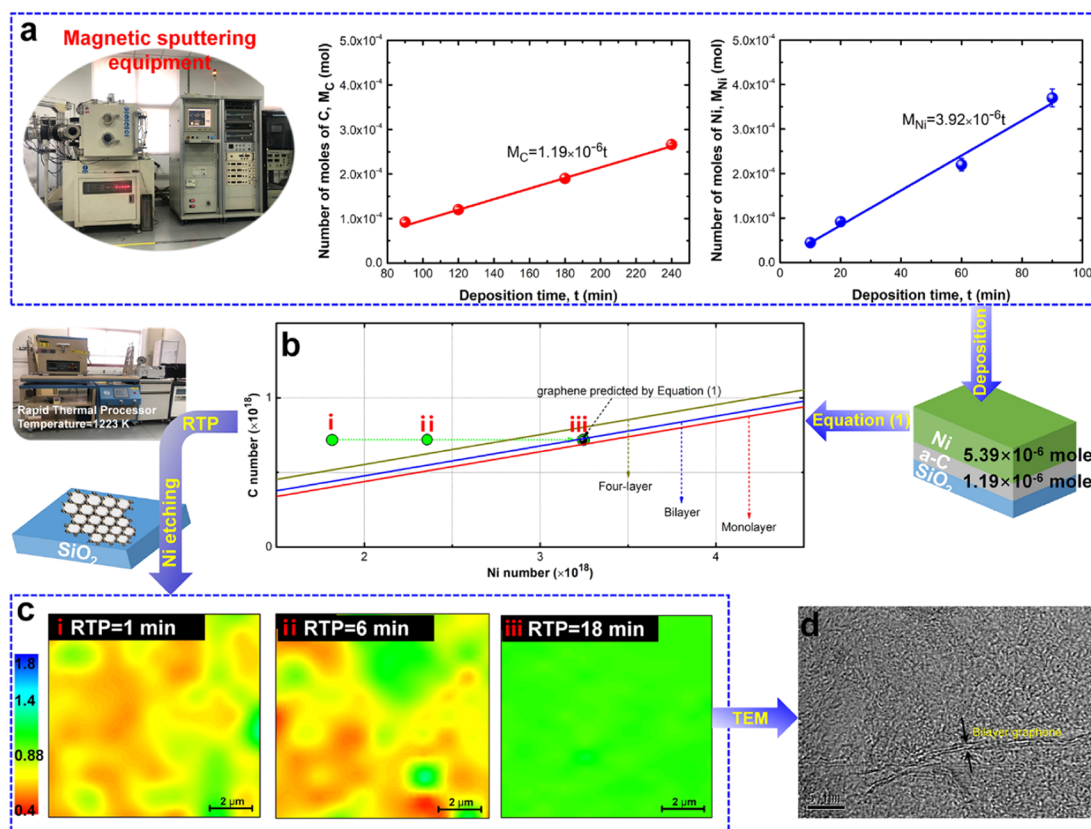


Figure 5. Experimental results for a-C-to-graphene transformation. (a) Number of moles of C and Ni atoms as a function of deposition time and fitting results in experiment, in which M_C and M_{Ni} in the inset equations are the number of moles of C and Ni, respectively (mole), and t is the deposition time (min). (b) Relationship between the number of C and Ni atoms and graphene for the experimental sample, and (c) Raman mapping of I_{2D}/I_G ratios in a $10 \mu\text{m} \times 10 \mu\text{m}$ region of the as-grown graphene on a SiO₂ substrate after RTP times of 1, 6, and 18 min, respectively. (d) HRTEM image of representative randomly chosen edges of the as-grown graphene for the sample at the RTP time of 18 min, which was taken using a TF-20 system with the graphene sample directly transferred onto a Cu-flat TEM grid.

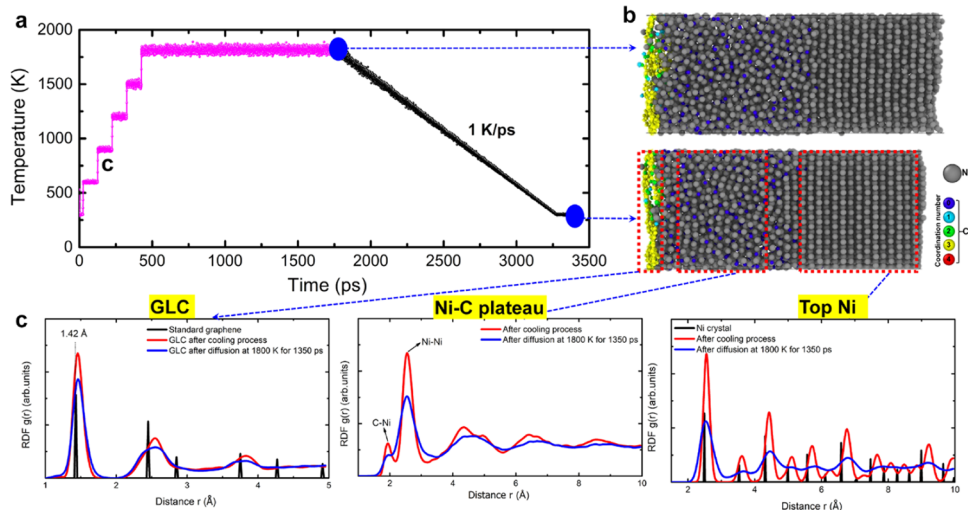


Figure 6. (a) Evolution of temperature during the cooling process. (b) Final morphologies of the Ni@a-C system obtained after diffusion at 1800 K for 1350 ps and the cooling process, respectively. (c) RDF spectra of GLC, C–Ni plateau, and top Ni regions in the Ni@a-C system after the cooling process, in which the results after diffusion at 1800 K for 1350 ps are also given for comparison.

identified by an I_{2D}/I_G ratio larger than 1.4; furthermore, an I_{2D}/I_G ratio between 0.8 and 1.4 corresponds to bilayer graphene.¹⁶ Hence, in Figure 5c, when the RTP time is 18 min, bilayer graphene with high uniformity and scale is generated, which is also confirmed by high-resolution transmission electron microscopy (HRTEM) in Figure 5d. This is highly

consistent with the result predicted by eq 1. In addition, the change in the I_{2D}/I_G ratio with RTP time (from 1 to 18 min) suggests the transformation of the graphene layer from a multilayer to a bilayer structure with high quality (light blue dots in Figure 5b), which can also be explained by eq 1, as shown in light blue dots of Figure 5b.

Although only one experimental example is provided and the experimental conditions can be further refined by increasing the RTP time or tailoring the a-C structure,²⁴ it is enough to convey that using eq 1 to design the Ni@a-C sample in experiment, we successfully realize the high-quality growth of RTP graphene with a goal-oriented structure and layers, and the RTP graphene layers can be controlled by making use of this universal eq 1, which is more practical for the subsequent technical applications. However, it is noted that the experimental RTP time (1, 6, and 18 min) is much larger than that (1350 ps) from the MD simulation, which can be attributed to the diversity of a-C and Ni structures and the difference in the dimension of the Ni@a-C system.¹⁸ Thus, the time dependence of the a-C-to-graphene transformation needs to be explored solely in experiment, but the effect of other factors (different a-C structures, Ni structures, Ni/C ratios, etc.) on the RTP growth of graphene in experiment can be explained by the fundamental relationship between the number of C and Ni atoms in eq 1. This not only simplifies the process parameters drastically but is also available for all kinds of C sources²⁴ and Ni structures.²⁶

3.4. Mechanism of a-C-to-Graphene Transformation during the RTP Process. It should be mentioned that Zheng,¹⁴ Wu,¹⁸ and Orofeo²¹ reported that the a-C dissolved into the metal catalyst at the heating stage and then precipitated from the solution upon cooling below the solid solubility limit to form the graphene, following the dissolution/precipitation mechanism. However, both calculation and experiment in the present work confirm that during the RTP process, a-C atoms diffuse into the Ni layer, but there are no C atoms expelled from the Ni layer after the cooling process and there is also no graphene formed at the top surface of the Ni layer, which coincides with the simulation by Chen²⁷ and experiments by Sun,⁴ Rodriguez-Manzo,¹⁵ Xiong,¹⁶ and Saenger.²²

Taking the system with a Ni/C ratio of 5/1 for example, after diffusion at 1800 K for 1350 ps, the cooling process from 1800 to 300 K (Figure 6a) was carried out at a cooling rate of 1 K/ps to investigate the effect of the cooling process on the diffusion and GLC quality. Figure 6b shows the final morphology of Ni@a-C systems after the cooling process, and that after diffusion at 1800 K for 1350 ps is also given for comparison. Note that after the cooling process, the whole system tends to be arranged orderly, which is confirmed by the RDF spectra of GLC, Ni–C plateau, and surplus Ni layers, as shown in Figure 6c. In particular, compared to the structure diffused at 1800 K for 1350 ps, the number of C atoms, which contributes to the formation of GLC, decreases to 363 from 406, indicating that during the cooling process, there are no C atoms precipitated from the C–Ni intermixing region. This is different from the Ni-catalyzed CVD growth of graphene, in which the segregation behavior of C atoms from the Ni catalyst occurs during the cooling process.^{32,33} In contrast, during the cooling process, the MSD increases first and then decreases gradually (Figure 7), resulting in the diffusion of more C atoms into the Ni layer. The MSD for Ni atoms gives a similar behavior to that for C atoms.

This demonstrates that during the RTP process, the nucleation and growth of graphene from a-C are mainly dominated by the diffusion behavior of C and the catalytic effect of Ni, rather than the CVD dissolution/precipitation mechanism;^{14,18,21} the graphitic C formation starts at low temperatures (>300 K), as shown in Figure 8, and the

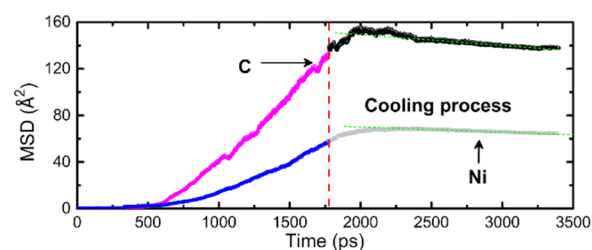


Figure 7. MSD with diffusion time during the cooling process. The results before diffusion at 1800 K for 1350 ps are also given for comparison.

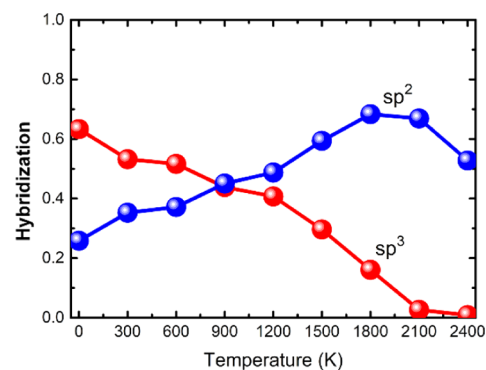


Figure 8. Evolution of sp^3 -C and sp^2 -C fractions in the a-C structure with temperature.

transformation of a-C into the thermodynamically more favorable graphene can be achieved still at the heating stage, such as 1800 K in calculation and 1223 K in experiment, confirmed by on-site microscopy analysis.¹⁵ In addition, compared to the experimental results, the existence of many holes and defects in simulated RTP GLC is attributed to the fast heating rate and short MD simulation time, which can be diminished by increasing the simulation time²⁷ or high-temperature annealing.^{34,35}

4. CONCLUSIONS

In this study, we combined RMD simulation and experiment to systematically explore the transformation of a-C into graphene in the RTP process. Based on the in-depth understanding of the diffusion behaviors of C atoms and structural transformation of a-C in systems at the atomic scale, results revealed that although a Ni–C plateau layer with a viscous liquid-like state and Ni/C ratio was observed in both simulation and experiment, it had no obvious influence on the growth of RTP graphene. Different Ni/C ratios in the Ni@a-C system affected the diffusion coefficient of C into Ni, leading to changes in the number of residual C atoms available for growing graphene, but the growth of RTP graphene was more sensitive to the change of a-C rather than the Ni layer. However, the effect of Ni and a-C thicknesses on the a-C-to-graphene transformation was fundamentally dominated by the relationship between the number of C and Ni atoms and the graphene structure, which could be conveyed by a new universal equation, and its universality and accuracy were confirmed by additional calculation with polycrystalline Ni and experiment. In addition, both calculation and experiments confirmed that the formation of graphene was mainly dominated by the diffusion behavior of C and the catalytic effect of Ni, rather than by the dissolution/precipitation

mechanism typically involved in Ni-catalyzed CVD growth of graphene. The present results give an accurate explanation for previous experiments and provide a scientific understanding of the a-C-to-graphene transformation. Most importantly, using this developed equation to design the experimental sample, fast synthesis of RTP graphene with high quality and desired layers on dielectric substrates can be realized through Ni-catalyzed transformation of various solid carbon sources (a-C, graphite, isolated graphene flakes, etc.), and the RTP process parameters can be simplified significantly, promoting the development of carbon materials for potential commercial applications.

■ ASSOCIATED CONTENT

📄 Supporting Information

The Supporting Information is available free of charge on the ACS Publications website at DOI: [10.1021/acs.jpcc.9b05143](https://doi.org/10.1021/acs.jpcc.9b05143).

Dependence of the a-C-to-graphene transformation on the Ni/C atomic ratio by tailoring the Ni layer; dependence of the a-C-to-graphene transformation on the C/Ni atomic ratio by tailoring the C layer; simulation of the effect of polycrystalline Ni on the a-C-to-graphene transformation (PDF)

■ AUTHOR INFORMATION

Corresponding Authors

*E-mail: lixw0826@gmail.com. Tel: 82-2-958-5450. Fax: 82-2-958-5451 (X.L.).

*E-mail: aywang@nimte.ac.cn. Tel: 86-574-8668-5710. Fax: 86-574-8668-5159 (A.Y.).

*E-mail: krlee@kist.re.kr. Tel: 82-2-958-5494. Fax: 82-2-958-5451 (K.R.L.).

ORCID

Xiaowei Li: [0000-0002-7042-2546](https://orcid.org/0000-0002-7042-2546)

Aiying Wang: [0000-0003-2938-5437](https://orcid.org/0000-0003-2938-5437)

Notes

The authors declare no competing financial interest.

■ ACKNOWLEDGMENTS

This research was supported by the Korea Research Fellowship Program funded by the Ministry of Science and ICT through the National Research Foundation of Korea (2017H1D3A1A01055070), the Nano Materials Research Program through the Ministry of Science and IT Technology (NRF-2016M3A7B4025402), the National Natural Science Foundation of China (51772307), the A-class pilot of the Chinese Academy of Sciences (XDA22010303), and the Ningbo Science and Technology Innovation Project (2018B10014).

■ REFERENCES

- (1) Lee, C.; Wei, X.; Kysar, J. W.; Hone, J. Measurement of the Elastic Properties and Intrinsic Strength of Monolayer Graphene. *Science* **2008**, *321*, 385–388.
- (2) Nair, R. R.; Blake, P.; Grigorenko, A. N.; Novoselov, K. S.; Booth, T. J.; Stauber, T.; Peres, N. M. R.; Geim, A. K. Fine Structure Constant Defines Visual Transparency of Graphene. *Science* **2008**, *320*, 1308.
- (3) Murali, R.; Yang, Y.; Brenner, K.; Beck, T.; Meindl, J. D. Breakdown Current Density of Graphene Nanoribbons. *Appl. Phys. Lett.* **2009**, *94*, No. 243114.
- (4) Sun, H.; Li, X.; Li, Y.; Chen, G.; Liu, Z.; Alam, F. E.; Dai, D.; Li, L.; Tao, L.; Xu, J. B.; et al. High-Quality Monolithic Graphene Films

via Laterally Stitched Growth and Structural Repair of Isolated Flakes for Transparent Electronics. *Chem. Mater.* **2017**, *29*, 7808–7815.

(5) Gong, J.; Liu, Z.; Yu, J.; Dai, D.; Dai, W.; Du, S.; Li, C.; Jiang, N.; Zhan, Z.; Lin, C. T. Graphene Woven Fabric-Reinforced Polyimide Films with Enhanced and Anisotropic Thermal Conductivity. *Composites, Part A* **2016**, *87*, 290–296.

(6) Zhang, L.; Chen, L.; Luo, H.; Zhou, X.; Liu, Z. Large-Sized Few-Layer Graphene Enables an Ultrafast and Long-Life Aluminum-Ion Battery. *Adv. Energy Mater.* **2017**, *7*, No. 1700034.

(7) Zhuang, H.; Deng, W.; Wang, W.; Liu, Z. Facile Fabrication of Nanoporous Graphene Powder for High-Rate Lithium-Sulfur Batteries. *RSC Adv.* **2017**, *7*, 5177–5182.

(8) Yi, M.; Shen, Z. A Review on Mechanical Exfoliation for the Scalable Production of Graphene. *J. Mater. Chem. A* **2015**, *3*, 11700–11715.

(9) Yang, W.; Chen, G.; Shi, Z.; Liu, C. C.; Zhang, L.; Xia, G.; Cheng, M.; Wang, D.; Yang, R.; Shi, D.; et al. Epitaxial Growth of Single-Domain Graphene on Hexagonal Boron Nitride. *Nat. Mater.* **2013**, *12*, 792–797.

(10) Hernandez, Y.; Nicolosi, V.; Lotya, M.; Blighe, F. M.; Sun, Z.; De, S.; McGovern, I. T.; Holland, B.; Byrne, M.; Gun'ko, Y. K.; et al. High-Yield Production of Graphene by Liquid-Phase Exfoliation of Graphite. *Nat. Nanotechnol.* **2008**, *3*, 563–568.

(11) Zhang, Y.; Zhang, L.; Zhou, C. Review of Chemical Vapor Deposition of Graphene and Related Applications. *Acc. Chem. Res.* **2013**, *46*, 2329–2339.

(12) Wu, T.; Liu, Z.; Chen, G.; Dai, D.; Sun, H.; Dai, W.; Jiang, N.; Jiang, Y. H.; Lin, C. T. A Study of the Growth-Time Effect on Graphene Layer Number Based on a Cu-Ni Bilayer Catalyst System. *RSC Adv.* **2016**, *6*, 23956–23960.

(13) Li, X.; Magnuson, C. W.; Venugopal, A.; Tromp, R. M.; Hannon, J. B.; Vogel, E. M.; Colombo, L.; Ruoff, R. S. Large-Area Graphene Single Crystals Grown by Low-Pressure Chemical Vapor Deposition of Methane on Copper. *J. Am. Chem. Soc.* **2011**, *133*, 2816–2819.

(14) Zheng, M.; Takei, K.; Hsia, B.; Fang, H.; Zhang, X.; Ferralis, N.; Ko, H.; Chueh, Y. L.; Zhang, Y.; Maboudian, R.; Javey, A. Metal-Catalyzed Crystallization of Amorphous Carbon to Graphene. *Appl. Phys. Lett.* **2010**, *96*, No. 063110.

(15) Rodríguez-Manzo, J. A.; Pham-Huu, C.; Banhart, F. Graphene Growth by a Metal-Catalyzed Solid-State Transformation of Amorphous Carbon. *ACS Nano* **2011**, *5*, 1529–1534.

(16) Xiong, W.; Zhou, Y. S.; Jiang, L. J.; Sarkar, A.; Mahjour-Samani, M.; Xie, Z. Q.; Gao, Y.; Ianno, N. J.; Jiang, L.; Lu, Y. F. Single-Step Formation of Graphene on Dielectric Surfaces. *Adv. Mater.* **2013**, *25*, 630–634.

(17) Barreiro, A.; Börrnert, F.; Avdoshenko, S. M.; Rellinghaus, B.; Cuniberti, G.; Rummeli, M. H.; Vandersypen, L. M. K. Understanding the Catalyst-Free Transformation of Amorphous Carbon into Graphene by Current-Induced Annealing. *Sci. Rep.* **2013**, *3*, No. 1115.

(18) Wu, Z.; Guo, Y.; Guo, Y.; Huang, R.; Xu, S.; Song, J.; Lu, H.; Lin, Z.; Han, Y.; Li, H.; et al. A Fast Transfer-Free Synthesis of High-Quality Monolayer Graphene on Insulating Substrates by a Simple Rapid Thermal Treatment. *Nanoscale* **2016**, *8*, 2594–2600.

(19) Robertson, J. Diamond-Like Amorphous Carbon. *Mater. Sci. Eng., R* **2002**, *37*, 129–281.

(20) Zhang, L.; Wei, X.; Lin, Y.; Wang, F. A Ternary Phase Diagram for Amorphous Carbon. *Carbon* **2015**, *94*, 202–213.

(21) Orofeo, C. M.; Ago, H.; Hu, B.; Tsuji, M. Synthesis of Large Area, Homogeneous, Single Layer Graphene Films by Annealing Amorphous Carbon on Co and Ni. *Nano Res.* **2011**, *4*, 531–540.

(22) Saenger, K. L.; Tsang, J. C.; Bol, A. A.; Chu, J. O.; Grill, A.; Lavoie, C. In Situ X-Ray Diffraction Study of Graphitic Carbon Formed during Heating and Cooling of Amorphous-C/Ni Bilayers. *Appl. Phys. Lett.* **2010**, *96*, No. 153105.

(23) Plimpton, S. Fast Parallel Algorithms for Short-Range Molecular Dynamics. *J. Comput. Phys.* **1995**, *117*, 1–19.

(24) Li, X.; Zhou, Y.; Xu, X.; Wang, A.; Lee, K. R. Role of the Carbon Source in the Transformation of Amorphous Carbon to

Graphene during Rapid Thermal Processing. *Phys. Chem. Chem. Phys.* **2019**, *21*, 9384–9390.

(25) Li, X.; Guo, P.; Sun, L.; Wang, A.; Ke, P. Ab Initio Investigation on Cu/Cr Codoped Amorphous Carbon Nanocomposite Films with Giant Residual Stress Reduction. *ACS Appl. Mater. Interfaces* **2015**, *7*, 27878–27884.

(26) Li, X.; Wang, A.; Lee, K. R. Transformation of Amorphous Carbon to Graphene on Low-Index Ni Surfaces during Rapid Thermal Processing: A Reactive Molecular Dynamics Study. *Phys. Chem. Chem. Phys.* **2019**, *21*, 2271–2275.

(27) Chen, S.; Xiong, W.; Zhou, Y. S.; Lu, Y. F.; Zeng, X. C. An Ab Initio Study of the Nickel-Catalyzed Transformation of Amorphous Carbon into Graphene in Rapid Thermal Processing. *Nanoscale* **2016**, *8*, 9746–9755.

(28) Li, X.; Li, L.; Zhang, D.; Wang, A. Ab Initio Study of Interfacial Structure Transformation of Amorphous Carbon Catalyzed by Ti, Cr, and W Transition Layers. *ACS Appl. Mater. Interfaces* **2017**, *9*, 41115–41119.

(29) Evans, D. J.; Holian, B. L. The Nose-Hoover Thermostat. *J. Chem. Phys.* **1985**, *83*, 4069–4074.

(30) Mueller, J. E.; van Duin, A. C. T.; Goddard, W. A., III Development and Validation of ReaxFF Reactive Force Field for Hydrocarbon Chemistry Catalyzed by Nickel. *J. Phys. Chem. C* **2010**, *114*, 4939–4949.

(31) Sinitisa, A. S.; Lebedeva, I. V.; Popov, A. M.; Knizhnik, A. A. Transformation of Amorphous Carbon Clusters to Fullerenes. *J. Phys. Chem. C* **2017**, *121*, 13396–13404.

(32) Mafra, D. L.; Olmos-Asar, J. A.; Negreiros, F. R.; Reina, A.; Kim, K. K.; Dresselhaus, M. S.; Kong, J.; Mankey, G. J.; Araujo, P. T. Ambient-Pressure CVD of Graphene on Low-Index Ni Surfaces Using Methane: A Combined Experimental and First-Principles Study. *Phys. Rev. Mater.* **2018**, *2*, No. 073404.

(33) Seah, C. M.; Vigolo, B.; Chai, S. P.; Ichikawa, S.; Gleize, J.; Normand, F. L.; Aweke, F.; Mohamed, A. R. Sequential Synthesis of Free-Standing High Quality Bilayer Graphene from Recycled Nickel Foil. *Carbon* **2016**, *96*, 268–275.

(34) Karoui, S.; Amara, H.; Bichara, C.; Ducastelle, F. Nickel-Assisted Healing of Defective Graphene. *ACS Nano* **2010**, *4*, 6114–6120.

(35) Jiao, M.; Song, W.; Qian, H. J.; Wang, Y.; Wu, Z.; Irle, S.; Morokuma, K. QM/MD Studies on Graphene Growth from Small Islands on the Ni(111) Surface. *Nanoscale* **2016**, *8*, 3067–3074.